Contents lists available at SciVerse ScienceDirect

NeuroImage

journal homepage: www.elsevier.com/locate/ynimg
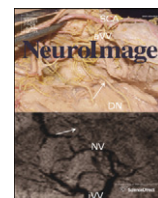
Evoked traveling alpha waves predict visual-semantic categorization-speed

Robert Fellinger [a], Walter Gruber [a,*], Andrea Zauner [a], Roman Freunberger [a,b], Wolfgang Klimesch [a]

[a] Department of Physiological Psychology, University of Salzburg, Austria
[b] Center for Lifespan Psychology, Max Planck Institute for Human Development, Berlin, Germany

ARTICLE INFO

ABSTRACT

In the present study we have tested the hypothesis that evoked traveling alpha waves are behaviorally significant. The results of a visual-semantic categorization task show that three early ERP components including the P1–N1 complex had a dominant frequency characteristic in the alpha range and behaved like traveling waves do. They exhibited a traveling direction from midline occipital to right lateral parietal sites. Phase analyses revealed that this traveling behavior of ERP components could be explained by phase-delays in the alpha but not theta and beta frequency range. Most importantly, we found that the speed of the traveling alpha wave was significantly and negatively correlated with reaction time indicating that slow traveling speed was associated with fast picture-categorization. We conclude that evoked alpha oscillations are functionally associated with early access to visual-semantic information and generate – or at least modulate – the early waveforms of the visual ERP.

Introduction

In EEG research an interesting and important question has been whether ongoing oscillations and event-related potentials (ERPs) represent independent phenomena. The best known example highlighting this question is the issue of phase reset. Whether ERPs are generated by fixed-latency/fixed-polarity responses or by a reset of ongoing oscillatory activity was and still is a hotly debated issue (see e.g. the pioneering work of Basar et al. and contributions from a variety of different laboratories, Barry et al., 2003; Basar Eroglu, 1999; Brandt, 1997; Fell et al., 2004; Fellinger et al., in press; Fuentemilla et al., 2006; Gruber et al., 2005; Krieg et al., 2011; Kruglikov and Schiff, 2003; Makeig et al., 2002; Mäkinen et al., 2005; Mazaheri and Jensen, 2006; Mazaheri and Picton, 2005; Ossandon et al., 2010; Penny et al., 2002; Risner et al., 2009; Ritter and Becker, 2009; Rizzuto et al., 2003; Shah et al., 2004; Yamagishi et al., 2003). Besides these two contrasting points of view there were others who pointed at the possibility of an interaction between both mechanisms (e.g. Min et al., 2007) plus it was also proposed that phase-reset particularly contributes to the generation of early (often called 'exogenous') potentials like the P1 and N1 whereas the later (termed 'endogenous') potentials are shaped by additive evoked mechanisms (Barry, 2009). For recent reviews see e.g., Klimesch et al. (2007c) and Sauseng et al. (2007).

Here we want to draw attention to the fact that the issue of phase-reset represents only a very specific aspect of the more general question of independence vs. interdependence between ERPs and ongoing oscillations. There are a variety of other issues that are of importance. As an example, the demonstration that early ERP components such as the C1, P1 and N1 'behave' like ongoing oscillations would be a strong support for a close interdependence between ERPs and oscillations. The early components C1, P1 and partly also the N1 are usually considered manifestations of a rather localized brain activity that can be described e.g. in terms of dipole source analysis (cf. e.g. Di Russo et al., 2002). This view, however, is questioned by findings showing that these components behave like a traveling alpha wave (e.g. Alexander et al., 2006; Klimesch et al., 2007a). Traveling waves are a phenomenon that is typical for ongoing oscillations, which has been reported early in EEG research (e.g. Adrian and Yamagiwa, 1935; Petsche and Marko, 1955) and which is meanwhile well documented (for reviews see e.g., Ermentrout and Kleinfeld, 2001; Hughes, 1995; Nunez, 2000; Nunez et al., 2001; Wu et al., 2008). Traveling waves represent a central aspect of physiological investigations showing the spreading of activity-waves over the cortex stemming from pulsating neurons (Adrian and Matthews, 1934; Freeman, 2004).

In the present study, we aim to extend the findings reported by Klimesch et al. (2007a) that early ERP components – and the P1 in particular – behave like a traveling alpha wave. Here we want to test a rather specific hypothesis that relates the (cognitive and physiological) functions of alpha to those of the expected alpha traveling wave. One central question is, whether traveling speed reflects a cognitive function that we have shown is closely associated with alpha: semantic processing and visual-semantic categorization in particular

(for reviews see Klimesch, 1997, 1999; Klimesch et al., 2007b). We therefore use a semantic picture categorization task which is embedded in a dual task paradigm. The reason to use in addition the latter type of paradigm is to make the task more difficult. Preliminary evidence based on unpublished pilot data suggests that topographical latency differences in early ERP components – which are a precondition to analyze traveling waves – are large when the task is difficult.

Our central hypothesis is that traveling speed should be correlated with semantic categorization-speed. What are the assumptions underlying this hypothesis? In an attempt to elaborate our hypothesis, we refer to a recently suggested theory ('the P1 inhibition timing theory', Klimesch, 2011) that tries to explain the cognitive and physiological meaning of the P1-component. With respect to the physiological function, the central idea is that the P1 – like ongoing alpha – reflects an inhibitory process which operates in two different ways depending on the type of task demands and processing requirements. In task relevant neural networks or brain regions, inhibition interacts with excitation and operates to increase the signal to noise ratio (SNR) by silencing neural activity with a comparatively low level of excitation. In task irrelevant and potentially competing networks or brain regions inhibition operates to suppress information processing. As an example for task relevant processes, we refer to findings showing that the P1 is increased over posterior brain regions when processing complexity is high (e.g. the P1 is larger for scrambled and/or inverted faces as compared to non-scrambled and/or upright faces, e.g., Allison et al., 1999; Itier and Taylor, 2004; Linkenkaer-Hansen et al., 1998). The interpretation of these and similar findings (cf. reviewed by Klimesch, 2011) is that an increase in the SNR which is associated with an increase in inhibition leads to an increase in the P1 amplitude. On the other hand, in tasks allowing for a dissociation between task relevant and task irrelevant brain regions – as is the case for tasks with hemifield presentations – the P1 tends to be larger over the task irrelevant ipsi – as compared to the task relevant contra-lateral recording sites (cf. Freunberger et al., 2008a; Klimesch, 2011; Mangun et al., 2001).

Based on these considerations we make the prediction that the P1 evoked traveling wave will be shaped by inhibition. As a consequence, the speed of spreading activation during early stimulus categorization will be reduced, if inhibition – associated with an increase in the SNR – will be increased. Because an increase in the SNR should enhance the quality of stimulus categorization and semantic classification, we expect a negative relationship between P1 travel speed and semantic classification time: low travel speed is linked to short and high travel speed to long classification times.

We also want to emphasize that the level of inhibition (which is modulated by alpha oscillations) may be controlled in a top down like manner. This means that the level of inhibition – which affects traveling speed – may be determined already in a pre-stimulus period. For a discussion of alpha as a top-down controlled processing mode see e.g. the recent review by Klimesch et al. (2011).

Method

Subjects

A sample of 19 subjects participated in the present experiment. Due to a high amount of artifacts (blinks and muscles) three subjects were rejected for further analyses. The final sample of 16 subjects consisted of 9 females and 7 males. Mean age was 22.9 years (SD 3.6 years). All subjects reported no neurological disorders or psychological pathologies and participated in the experiment after giving informed consent. Subjects received 10 Euro as participation-fee.

Task

We used a dual task paradigm, a (semantic) categorization and recognition task. In the categorization task subjects were asked to indicate whether a picture represented a landscape or building and – in addition – to remember or not-remember the picture (depending on information provided by a cue). In the recognition task 80 pictures presented in the categorization task were shown together with a set of 80 new pictures (distracters) in a random sequence. In the present study only the data of the categorization task were analyzed.

The categorization task started with a cue that consisted either of a symbol with, 'thumbs up or ,thumbs down'. Thumbs up indicated that the upcoming picture must be categorized and remembered whereas thumbs down indicated that the picture must be categorized only. We use the term 'target' for pictures that must in addition be remembered and 'non-target' for pictures that must not be remembered. Subjects were told to respond as fast as possible by a button press (with the right index or middle finger) whether the picture represents a building or landscape. Task demands and the structure of a single trial are illustrated in Fig. 1.

The categorization task was performed in two counterbalanced blocks. In one block the stimulus onset time (SOT) was fixed with a duration of 1300 ms, in the other block SOT varied between 1300 +/− 175 ms (i.e. between 1125 and 1475 ms). The cue offset coincided with the onset of the picture presentation, which lasted for 2000 ms. A total of 360 pictures were used consisting of 180 landscape- and 180 building-scenes. In each block 180 pictures (90 landscapes and 90 buildings) were presented. The physical properties of all pictures were kept constant by adjusting the luminance, contrast and magnitude spectra (to the overall averages of all used pictures). The average magnitude spectrum was integrated with the corresponding phase spectrum of each picture (for an equal procedure please see Philiastides et al., 2006). Randomized between trials, half of the pictures were cued with a 'remember', the other half with a 'non-remember'-cue. Before and after the experimental task the EEG was recorded during two resting conditions (eyes-open, eyes-closed) for two minutes.

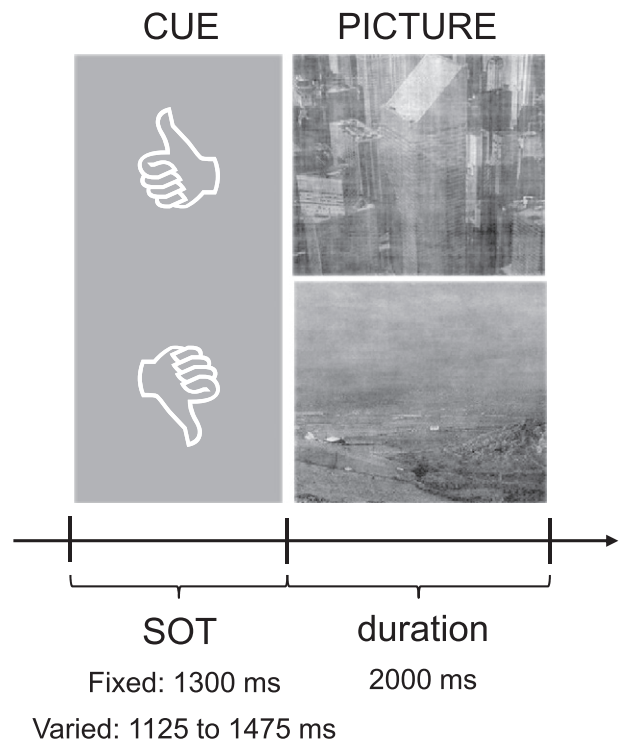**Fig. 1.** Experimental design. After the presentation of a cue that forced subjects either to remember or not-remember the upcoming item the relevant picture appeared. This picture should always be categorized as accurate and fast as possible into two different categories: either as a landscape or a building. The stimulus-onset-time (SOT) was either fixed or varied (block-design, counter-balanced between subjects).

Data acquisition

EEG signals were recorded from 60 active scalp-electrodes (Ag–AgCl-electrodes) referenced against a nose electrode and mounted according to the 10–20-system using an electrode cap (EasyCap, Inc., Herrsching, Germany). The signals were amplified using a BrainAmp amplifier (Brain Products, Inc., Gilching, Germany) with a sampling rate at 1000 Hz. In order to reduce AC line artifact a notch filter was set at 50 Hz and recording bandwidth was set from 0.15 to 100 Hz. In order to control for eye-movements, two electrodes were set at horizontal and vertical positions near the right eye.

Data-analysis

All basic processing steps were performed with BrainVisionAnalyzer 2.01 (Brain Products, Inc., Gilching, Germany). At first the data were re-referenced to the earlobe-electrodes and broadly filtered between 0.5 and 70 Hz. Then data were manually checked for muscle- and corrected for eye-blinked artifacts by applying an ICA-ocular-correction. Single-trial phase-analyses were done with custom-made codes in Matlab (The MathWorks, Inc., MA, USA). The topographical voltage-plots in Fig. 2B were created with the open-source Matlab-toolbox 'Fieldtrip' (Oostenveld et al., 2011).

Pre-stimulus alpha power

As we wanted to use as many trials as possible for our specific analyses (in order to increase the signal-to-noise-ratio, especially necessary for phase-analysis) we intended to collapse all data. Thus, we checked for differences in pre-stimulus whole-power between conditions as it is known that it can have various effects on post-stimulus event-related processes (e.g. Brandt and Jansen, 1991; Rajagovindan and Ding, 2010). Therefore we did a respective pre-analysis and calculated the average alpha-power (8 to 10 Hz) in a time-interval ranging from -500 to -100 prior to the onset of the picture.

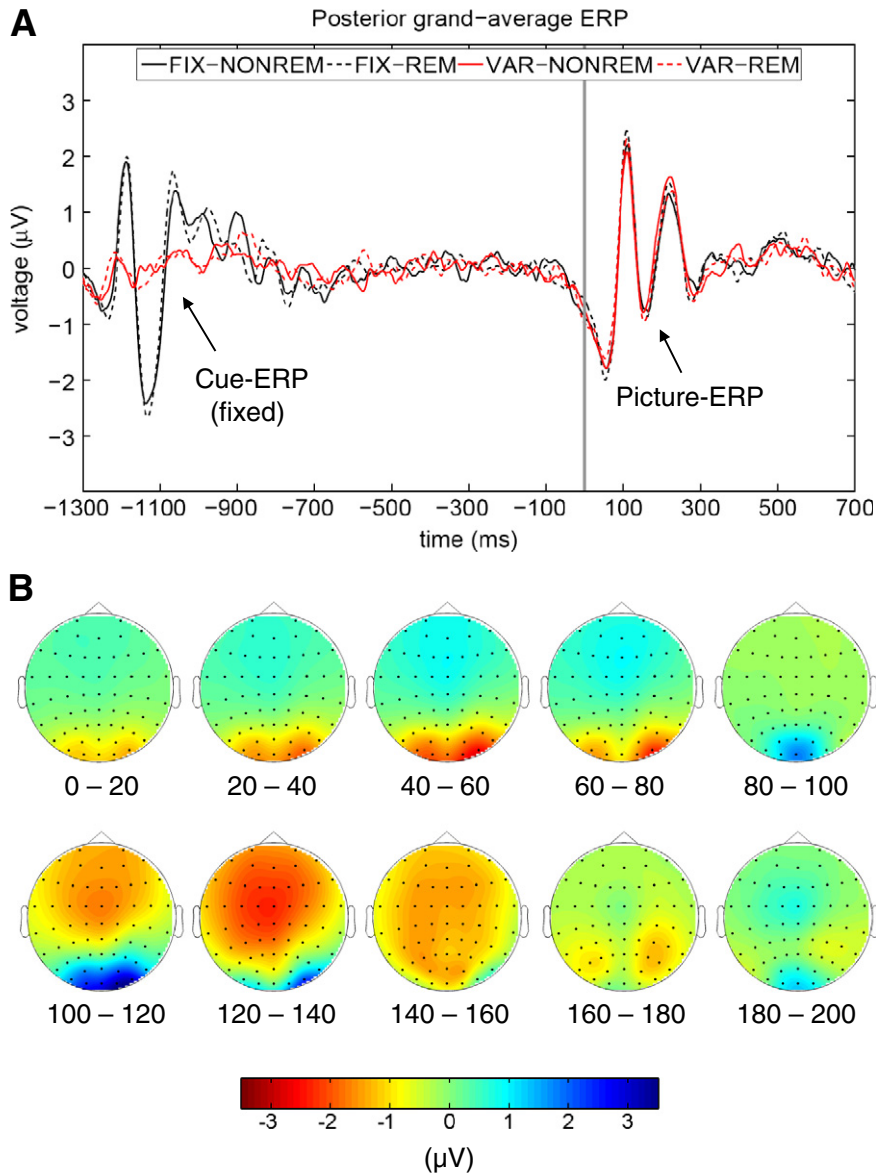**Fig. 2.** Posterior ERPs and voltage distributions. A) Posterior grand-average ERPs for the four different experimental conditions are depicted (averaged across the five electrodes of interest). Both stimuli (cue and picture) elicited an alpha-shaped, early evoked ERP-complex. B) The voltage maps display the grand-averages across all conditions during the first 200 ms post-stimulus (picture) in 20 ms steps.

Individual alpha frequency (IAF)

Previous studies showed that the dominant alpha-frequency can vary substantially between subjects which results in different frequency-characteristics of the EEG-signal (Klimesch, 1997). In order to avoid this we descriptively checked the sample for homogeneity concerning IAF. Therefore we segmented all resting-conditions into consecutive 2000 ms segments and applied a Fast-Fourier-Transformation (FFT). After averaging the average for the five posterior electrodes PO7, O1, Oz, PO8 and O2 was calculated.

ERP-latencies

For ERP-analyses the data were band-pass-filtered in a frequency-range between 4 and 20 Hz. Then data were segmented centered to stimulus presentations in a time-window ranging from −1400 to 600 ms. After averaging single-trials the individual ERP-components were semi-automatically detected. For detecting the N50 we searched for the negative peak in the time-window from 30 to 80 ms, for the P1 for the positive peak between 80 and 140 ms and for the N1 once again for the negative peak between 150 and 200 ms.

ERP-traveling-characteristic (ERP-TC)

In order to quantify the traveling of the ERP-complex we established an index we named ERP-traveling-characteristic (ERP-TC). The rationale behind this parameter is that traveling results in a constant delay in ERP-latencies within a certain direction. The calculation of the difference between the latencies of the lateral electrodes minus the central electrodes (for the two electrode pairs O2/Oz and PO8/O2) should lead to positive values. The more systematic and the larger latency-differences are the higher the positive values will be. Therefore we applied the following formula to the three ERP-components:

$$
\begin{aligned}
\text{latdiff}_1\left(s_i, c_j\right) &= \text{lat}_{O2}\left(s_i, c_j\right) - \text{lat}_{Oz}\left(s_i, c_j\right) \\
\text{latdiff}_2\left(s_i, c_j\right) &= \text{lat}_{PO8}\left(s_i, c_j\right) - \text{lat}_{Oz}\left(s_i, c_j\right) \\
\text{latdiff}_{Total}\left(s_i, c_j\right) &= \text{latdiff}_1\left(s_i, c_j\right) + \text{latdiff}_2\left(s_i, c_j\right) \\
&= \left[\text{lat}_{O2}\left(s_i, c_j\right) - \text{lat}_{Oz}\left(s_i, c_j\right)\right] + \left[\text{lat}_{PO8}\left(s_i, c_j\right) - \text{lat}_{Oz}\left(s_i, c_j\right)\right] \\
&= \text{lat}_{PO8}\left(s_i, c_j\right) - \text{lat}_{Oz}\left(s_i, c_j\right)
\end{aligned} \tag{1}
$$

where s_i = the i'th subject, c_j = the j'th component (with $j_1 = N_{50}, j_2 = P_1, j_3 = N_1$), latdiff = latency difference between respective components, lat = latency.

In order to get a parameter that indexes the traveling-characteristic of the whole ERP-complex (comprising all three components) we z-transformed the values obtained for every component between subjects and averaged the resulting values for all three components:

$$
\begin{aligned}
\overline{c}_j &= \frac{\sum_{i=1}^{N} \text{latdiff}_{Total}\left(s_i, c_j\right)}{N} \\
z\left(s_i, c_j\right) &= \frac{\text{latdiff}_{Total}\left(s_i, c_j\right) - \overline{c}_j}{\text{std}\left(c_j\right)} \\
\text{ERP}_{TC}(s_i) &= \frac{\sum_{j=1}^{3} z\left(s_i, c_j\right)}{3}.
\end{aligned} \tag{2}
$$

Phase-delay: single trial peak and trough detection

The EEG was segmented as described for the ERP-analyses but then the single-trial data (for three right-parietal electrodes Oz, O2 and PO8) were transformed into time-frequency matrices by using a Gabor-transformation (0.5 Hz frequency steps). The phase values – obtained for each sample point and frequency step – were subjected to a simple classification algorithm that was used to detect peaks

and troughs. Phase angles were categorized into four quadrants and for each sample-point and frequency step it was determined whether the observed phase angle fell in the peak or trough quadrants.

The respective quadrants were defined as 90° sectors at the unit circle around the respective phase angles reflecting the peak and the trough. The peak quadrant was defined as the phase-range between 315 and 45° and the trough quadrant as those phases between 135 and 225°. On the basis of this classification algorithm we determined the number of cases falling in the peak and trough quadrant. Thus, we obtained two frequency distributions for each subject, sample point and frequency step, one for 'peaks' and the other for 'troughs'. Then we transformed the frequencies by using the following formula (for details concerning the phase-analysis please see the Supplementary Figures S1, S2):

$$
\begin{aligned}
&h(\text{subj}_i, \text{trial}_k, \text{time}_m, \text{freq}_n) \\
&= \begin{cases} 1 & \text{if } 45° \geq \varphi(\text{subj}_i, \text{trial}_k, \text{time}_m, \text{freq}_n) \geq 315° \text{ (peak)} \\ 1 & \text{if } 135° \leq \varphi(\text{subj}_i, \text{trial}_k, \text{time}_m, \text{freq}_n) \leq 225° \text{ (trough)} \\ 0 & \text{else} \end{cases}
\end{aligned} \tag{3}
$$

$$
\begin{aligned}
h_{rel}(\text{subj}_i, \text{time}_m, \text{freq}_n) &= \frac{\sum_{k=1}^{K} h(\text{subj}_i, \text{trial}_k, \text{time}_m, \text{freq}_n)}{K} \\
\overline{h}_{rel}(\text{subj}_i, \text{freq}_n) &= \frac{\sum_{m=1}^{M} h_{rel}(\text{subj}_i, \text{time}_m, \text{freq}_n)}{M} \\
z_{h_{rel}}(\text{subj}_i, \text{time}_m, \text{freq}_n) &= \frac{h_{rel}(\text{subj}_i, \text{time}_m, \text{freq}_n) - \overline{h}_{rel}(\text{subj}_i, \text{freq}_n)}{\text{std}(h_{rel}[(\text{subj}_i, \text{time}_m, \text{freq}_n)])}
\end{aligned} \tag{4}
$$

where s_i = the i'th subject, T_k = the k'th trial, t_m = the m'th time-point, f_n = the n'th frequency.

The obtained waveforms were normalized frequency distributions for peaks and troughs that can be interpreted in a similar way as can be done for a probability function. The waveforms reflect the likelihood of an appearance of peaks and troughs over time.

The reason for using this classification procedure was to compensate for jitters in phase. For real data the distribution of phase values over time rarely shows a regular 0 to 360° ramp-like structure but instead quite frequently an irregular development with 'jumps' in phase is the case. The disadvantage of our method is that – in ideal cases – information about the exact appearance of a peak or trough is smeared in the order of the length of the categorization period which is 25 ms (i.e., a quarter of a period) for a frequency of 10 Hz. The critical question, thus, was whether this method would allow to predict the appearance of early ERP components and their topographic latency delays.

In order to test for the assumption that the obtained waveforms exhibit a systematic topographic phase-delay across subjects we calculated cross-correlations between the electrode-pairs Oz/O2 and O2/PO8 for every frequency and every subject within a time-window of 0 (picture-onset) to 200 ms post-stimulus. Positive lag values were associated with delayed peaks or troughs at O2 (relative to Oz) and PO8 (relative to O2) respectively. Negative values indicated a shift in the opposite direction. We calculated the cross-correlations for the two electrode pairs (Oz, O2 and O2, PO8), the two probability distributions (for peaks and troughs) and the two SOT-conditions (varied and fixed). This resulted in eight matrices for every subject. By averaging the obtained lag values for peaks and troughs, we obtained estimates for phase delays between the following four frequencies of interest (FOI): theta (4–6 Hz), alpha1 ('lower alpha', 8–10 Hz), alpha2 ('upper alpha', 10–12 Hz) and beta (16–18 Hz).

Statistical analyses

Pre-stimulus alpha-power

We checked for differences in pre-stimulus alpha-power between conditions by applying three repeated-measures ANOVAs with the factors SOT (FIXED vs. VARIED) and TASK (REMEMBER vs. NON-REMEMBER). This pre-testing was done for the electrodes Oz, O2 and PO8 which were later used for calculating the phase-delay (see Data acquisition section).

Individual alpha frequency (IAF)

The peak-frequency of the power-spectrum was visually evaluated for each subject in every resting-condition. Afterwards the mean across all conditions was calculated in order to get an overall resting-IAF.

ERP-latencies

In order to quantify the statistical significance for ERP-latencies we applied three repeated-measure ANOVAs (for the ERP-components N50, P1 and N1) with the factors ELECTRODE (PO7, O1, Oz, O2, PO8), SOT (FIXED vs. VARIED) and TASK (REMEMBER vs. NON-REMEMBER). In order to check for selective differences in ERP-latencies between consecutive electrodes paired-sample t-tests were applied to the respective mean-values (averaged across the two conditions). To test for a possible relationship between the ERP-TC and the categorization speed, Spearmen correlations between these variables were calculated.

Phase-delay

In order to test for significant delays we calculated one-sample t-tests (deviation from zero) for every FOI. In addition we checked if there were significant differences in delays between FOI by calculating a repeated-measure ANOVA with the factor FOI (theta, lower alpha, upper alpha, beta). Statistical post-hoc testing for differences between pairs of FOIs was done with paired-sample t-tests. In addition, we tested for relationships between the respective delay values of each FOI, reaction-time and ERP-TC by calculating Spearman-correlations. Finally we applied a hierarchical cluster-analysis (between-groups linkage, squared Euclidean distance, the cluster-solution was chosen preceding the greatest step in Euclidean distance) to the phase-delay data in the lower alpha range (as for this FOI the most effects were prominent) in order to find possible sub-groups of subjects with distinct phase-delays.

Results

Behavioral data

In the categorization task overall performance consisted of 96% correct responses (fixed condition, remember: 95%, non-remember: 97%; varied condition, remember: 96%, non-remember: 96%). Average reaction time was 793 ms (fixed condition, remember: 812 ms, non-remember: 793 ms; varied condition, remember: 791 ms, non-remember: 774 ms). There were no statistically significant effects between experimental conditions, neither for categorization accuracy nor for categorization-speed (reaction-time).

Recognition performance showed an overall very low mean value of 53% recognized pictures (fixed: 52%, varied: 53%). Calculation of d′ showed a mean value of 0.23 (fixed: 0.15, varied: 0.31). The percentage of recognized pictures did not vary between the fixed and varied condition as assessed by paired-sample t-tests. However, a significant difference was found for d′ ($p < 0.05$) which was most likely due to a higher false-alarm rate in the fixed condition.

Pre-stimulus alpha power

None of the conducted ANOVAs revealed a significant effect. Therefore we conclude that a differential pre-stimulus effect of the task-specific manipulations on post-stimulus processing is very unlikely.

Individual alpha frequency (IAF)

The descriptive evaluation showed that the mean IAF was at 10.15 Hz and standard-deviation was 0.55 Hz. As the variance between subjects was only at around a half Hertz it can be concluded that there was a high homogeneity between subjects concerning IAF.

ERP-latencies

As depicted in Fig. 2 the ERPs exhibited a pronounced posterior P1–N1 wave in response to both of the stimuli, the cue and the picture. It was preceded by an early negative component which we termed N50 (a negative component with a latency of around 50 ms). These three components, the N50, P1 and N1 formed a wave complex with a clear frequency characteristic in the alpha range as can be inferred by inter-peak latencies (mean inter-peak latencies between N50 and N1 were: 111 ms for cues and 109 ms for pictures).

Cue

As shown in Fig. 3A, mean latency differences for the three components – collapsed over all task conditions – were small. Statistical analyses (based on 3-way repeated measure ANOVAs with the factors ELECTRODE, SOT and TASK) revealed no significant effects for the N50 component, but a significant ELECTRODE × SOT interaction ($F_{4/60} = 3.78$, $p < 0.05$) for the P1 and a significant ELECTRODE × TASK interaction ($F_{4/60} = 3.49$, $p < 0.05$) for the N1 in addition to a main effect for ELECTRODE ($F_{4/60} = 3.48$, $p < 0.05$). The post-hoc comparison revealed that there was a significant difference in latency between O1 and PO7.

Inspection of the respective P1 latency means for the significant ELECTRODE × SOT interaction showed a comparatively flat topographical distribution for the varied condition. In the fixed condition P1 latencies were shorter at PO7 and O1 and longer at Oz, O2 and O8 (as compared to the respective values in the varied condition). For the N1 latencies, the main effect for ELECTRODE reflected the large differences between O1 and PO7 (with the shortest and largest latencies of 186 ms and 176 ms respectively). The significant interaction showed that latencies were shorter in the NON-REMEMBER (compared to the REMEMBER condition), but only at O1 and Oz (thereby exhibiting a pronounced U-shaped profile between PO7, O1, Oz, O2 and PO8).

In summary, for cues there was a weak tendency of a left hemispheric 'advantage' centered around O1 to exhibit shorter latencies for the fixed condition (reflected by the P1) and the NON-REMEMBER condition (reflected by the N1). These findings can also be observed in the collapsed data depicted in Fig. 3A. They were weakly evident for the P1, but comparably pronounced for the N1.

Picture

Inspection of the latency differences for pictures revealed that for all of the three components, peak latencies were generally shortest at Oz and longest at PO8 (cf. Fig. 3B). Statistical analyses showed a significant main effect for ELECTRODE for all of the three components. N50: $F_{4,60} = 3.70$, $p < 0.05$; P1: $F_{4,60} = 6.25$; $p < 0.01$; N1: $F_{4,60} = 10.15$, $p < 0.01$. This finding demonstrates that there were systematic and significant latency differences between electrodes for all of the three components.
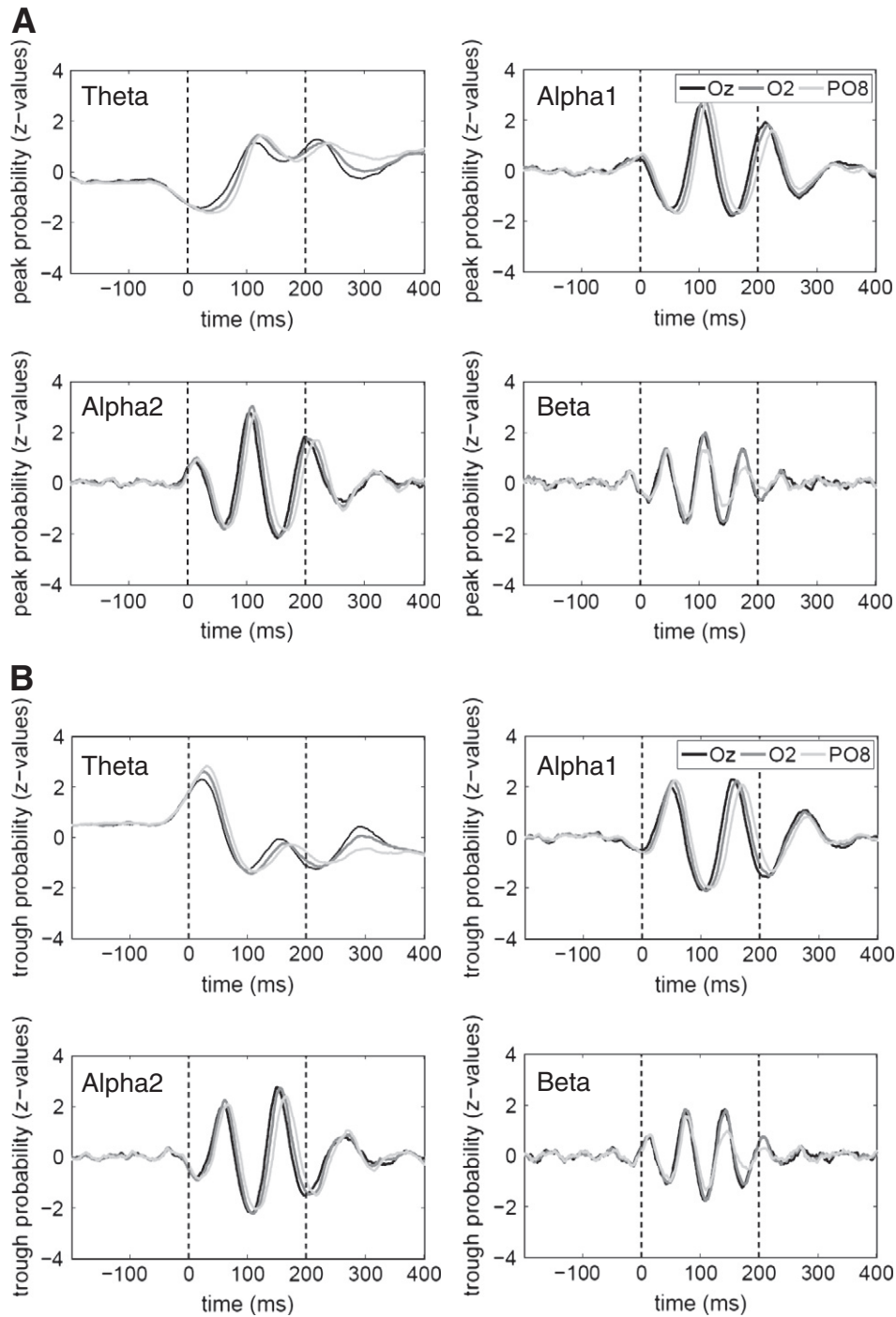
Fig. 3. ERP-latency differences between electrodes. A) These bar-graphs depict the post-hoc testing (main-effect ELECTRODE) for the cue (all three components). Clear and systematic latency-shifts were not observable. B) Here the same as in Fig. 3A but now for pictures (which had to be categorized) is displayed. As can be seen the latencies for N50, P1 and N1 were increased systematically from Oz to PO8. Additionally there was an increase in N1-latency from Oz to PO7. (* = p<0.05, ** = p<0.01). Error bars represent the respective confidence-intervals.

N50 latencies were not affected by task variables, as the lack of main effects or significant interactions with SOT and TASK indicated. In contrast, P1- and N1 latencies are affected by both task variables. For the P1, the following interactions reached significance, ELECTRODE× SOT ($F_{4/60} = 4.36$, p<0.05), ELECTRODE× SOT×TASK ($F_{4/60} = 3.19$, p<0.05). N1-latencies exhibited an influence of TASK, which was revealed by the interaction ELECTRODE×TASK ($F_{4/60} = 3.81$, p<0.05).

Inspection of the respective means of the 3-way interaction for the P1 showed shorter latencies for the varied condition but only at Oz and O2, which in addition were shorter (particularly at these sites) for NON-REMEMBER as compared to REMEMBER. The N1 featured a similar effect for Oz and O2 where latencies were shortest in the NON-REMEMBER as compared to REMEMBER.

In summary, for pictures there was a tendency of the P1 for a midline and right hemispheric 'advantage' centered on Oz and O2 to exhibit shorter latencies for both the varied and NON-REMEMBER condition. For the N1 a similar tendency was found, but for the NON-REMEMBER condition only. The overall pattern of these findings was clearly evident in the mean latencies that are collapsed over task conditions as shown in Fig. 3B.

Correlation between the ERP-traveling-characteristic (ERP-TC), categorization-speed (reaction-time) and peak latencies

The correlation between the ERP-TC and categorization speed (as measured by RTs) showed a significant negative relationship ($r_{ERP-TC, cat.-speed} = -0.549$, p<0.05). As the scatter plot in Fig. 5A illustrates, this finding indicates that longer mean latency differences between Oz, O2 and PO8 (reflecting slow traveling speed) were associated with shorter RTs (reflecting faster categorization speed).

As depicted in Table 1, none of the peak latencies (N50, P1 and N1) correlated significantly with categorization-speed. Significant correlations, however, were found between peak latencies (for N50 at Oz and O2 and for P1 at Oz), indicating that strong effects in inter-peak latencies (large ERP-TC values) were associated with short latencies at the leading electrode Oz.

Phase-delay: traveling alpha waves

The normalized frequency distributions for peaks and troughs are depicted in Fig. 4. They showed a large increase in the concentration of peaks (Fig. 4A) and troughs (Fig. 4B) post-stimulus. Most importantly, a

Table 1
Correlations. Relevant correlations between categorization-speed (cat.-speed), ERP-traveling-characteristic (ERP-TC), absolute ERP-latencies ('component'/'electrode') and frequency of interest phase-delays (PD) (bold numbers mark significant effects).

	Cat.-speed	ERP-TC	N50/Oz	N50/O2	N50/PO8
Cat.-speed		**−0.549***	0.340	0.337	0.177
ERP-TC	**−0.549***		**−0.776****	**−0.740****	−0.394
	P1/Oz	P1/O2	P1/PO8	N1/Oz	N1/O2
Cat.-speed	0.185	0.141	−0.012	0.131	0.140
ERP-TC	**−0.505***	−0.171	−0.021	−0.412	−0.278
	N1/PO8	PD-theta	PD-alpha1	PD-alpha2	PD-beta
Cat.-speed	−0.206	−0.308	**−0.586***	**−0.582***	−0.478
ERP-TC	0.087	0.355	**0.797****	**0.845****	0.454

* p<0.05.
** p<0.01.

Fig. 4. Frequency-distributions for peak and troughs as a function of time. A) In this graphic the normalized frequency-distribution for the three right posterior electrodes (for all frequencies of interest) is shown. Note that there is a prominent increase in z-values during the time-window of the P1 especially in the alpha-range (reflecting increased phase-stability). The prominent shifts between the lines are caused by systematic phase-shifts from Oz to O2 and from O2 to PO8. B) This graph displays the same as Fig. 4A but here the results are shown for troughs. High z-values are observable particularly in the time-window of the two negative components N50 and N1 (in the alpha range too). Once again, note the shifts reflecting systematic phase-delays from occipital midline to the right parietal area.

coincidence of peaks and troughs with the N50, P1 and N1 could be observed for the two alpha bands, but not for theta and beta.

The results of t-tests – which were calculated to test for significant phase-delays – revealed a systematic shift (with a significant deviation from zero) for all FOIs: theta ($t_{15} = 3.53$, $p < 0.01$), lower alpha ($t_{15} = 5.28$, $p < 0.001$), upper alpha ($t_{15} = 5.48$, $p < 0.001$), beta ($t_{15} = 2.54$, $p < 0.05$). As only positive shifts were observed we can conclude that all FOIs exhibit a shift from posterior to more lateral

sites. The respective mean values were, theta = 2.2 ms, lower alpha = 4.2 ms, upper alpha = 3.5 ms, beta = 0.9 ms. The repeated-measure ANOVA showed a significant effect for differences in delays between FOIs ($F_{3/45} = 9.72$, $p < 0.001$). The applied paired-sample t-tests confirmed differences for the following FOI-comparisons: theta/lower alpha ($t_{15} = -3.09$, $p < 0.01$), lower alpha/upper alpha ($t_{15} = 2.77$, $p < 0.05$), lower alpha/beta ($t_{15} = -3.98$, $p < 0.001$), upper alpha/beta ($t_{15} = 4.139$, $p < 0.001$). As depicted in
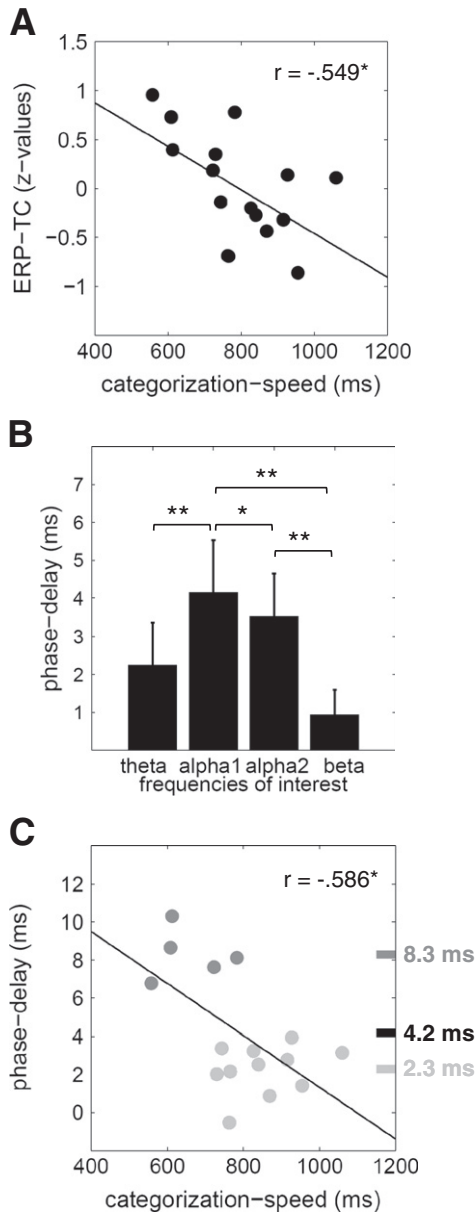
Fig. 5. Main results. A) The scatter plot depicts the negative correlation between ERP-traveling-characteristic and categorization-speed (r = − 0.549, p<0.05). This relationship suggests that larger latency-shift in the ERP-complex from Oz to PO8 was associated with fast picture-categorization. B) Here mean phase-delays for all frequencies of interest are depicted. The positive mean phase-delays indicate a systematic shift from midline occipital to more right parietal sites. Testing for differences between frequencies revealed that alpha1 ('lower alpha', 8–10 Hz) was the frequency with the highest delay and the only one that differed from all other frequencies (indicated by the asterisks; *p<0.05, **p<0.01). Error bars represent the respective confidence-intervals. C) In this graph the relationship between phase-delay and categorization speed is shown. The plot including all points displays the negative correlation between these two variables (r = − 0.586, p<0.05). An applied cluster-analysis suggested that there were two subgroups in the sample: one with a comparatively high delay (dark gray points, mean = 8.3 ms) and one with a low phase-delay (light gray points, mean = 2.3 ms).

Fig. 5B, these findings show that the phase-delay of lower alpha oscillations is significantly higher than those of all other frequencies. The mean value of 4.05 ms corresponds nicely to the observed ERP-latency delays (cf. Fig. 3B), which vary around 4.5 ms for the same distance (cf. traveling-speed in meter/second is almost the same).

With respect to the relationship between phase-delays and reaction-times, we obtained the following significant correlations: $r_{alpha1, \text{ reaction time}} = -0.586$ (p<0.05), $r_{alpha2, \text{ reaction time}} = -0.582$

(p<0.05). Inspection of the scatter plot shown in Fig. 5C suggests two clusters of subjects with small and comparatively large delay value (cf. the light and dark data points in Fig. 5C). The results of the cluster-analysis confirmed this observation and led to the extraction of two different sub-groups with different phase-delays in the lower alpha range (Euclidean distance = 6.81): one subgroup (consisting of 11 subjects) with a mean phase-delay of 2.3 ms and another group (comprising 5 subjects) with a mean of 8.3 ms. This finding suggests that phase-delays were not gradually distributed across subjects, but rather exhibited a bimodal-distribution that resulted in the distinction of two subgroups.

For the alpha range the obtained phase delays were highly correlated with the ERP-TC (alpha1: r = 0.797, p<0.001; alpha2: r = 0.845, p<0.001). This suggests that the topographical latency delays in the ERP are closely associated with the respective peak latencies in the alpha-range. This argument is strengthened by the fact that all other FOIs displayed no significant correlation with respect to ERP-TC (cf. Table 1).

Discussion

The obtained findings confirmed that early ERP components in a visual-semantic judgment task with a latency range of about 50 to 200 ms post-stimulus had a dominant frequency characteristic in the alpha range and behaved like traveling waves do. They exhibited a traveling direction from midline occipital to right lateral parietal sites. Most importantly, the speed of the traveling alpha wave was negatively correlated with reaction time indicating that slow traveling speed was associated with picture-categorization. This latter finding relates evoked traveling alpha waves to the recently discussed, functional role of alpha-oscillations particularly for perceptual (e.g. Babiloni et al., 2006; Busch et al., 2009; Hanslmayr et al., 2007; Mathewson et al., 2009; Rihs et al., 2007; Romei et al., 2010; Thut et al., 2006) and semantic processing (e.g. Freunberger and Klimesch, 2008; Freunberger et al., 2008b; Mima et al., 2001; Vanni et al., 1997). The general idea is that evoked alpha waves reflect an active process that enables controlled access to stored information in memory and thereby 'extracts' the meaning of sensory information. This is crucial as the meaning of sensory information is not represented by a stimulus itself — it is represented in our memory (Klimesch et al., 2011).

The dominant alpha characteristic of the ERPs can already be judged by visual inspection (cf. Fig. 2) and could not be observed only for the judgment task but also in response to the presentation of a cue preceding task performance. This may indicate that evoked alpha waves reflect a task specific processing mode that controls the encoding of visual information (for a review see Klimesch et al. (2011)). During the encoding of the cue and pictures three prominent components were observed consisting of an early negative component around 50 ms (which we termed N50), the P1 and N1. Inter-peak latencies between the N50 and N1 varied closely around 110 ms and thus the ERP wave consisting of these three components reflect evoked alpha activity with a frequency around 9 Hz.

Significant and topographically related latency differences for all of these three components were found during the categorization task only. As illustrated in Fig. 3B, the latency differences were largest between Oz and PO8, suggesting a travel direction from medial occipital to right lateral parieto-occipital sites. Most interestingly, this travel direction (as estimated on the basis of latency differences) was identical for the N50, P1 and N1 with the single exception that the N1 shows in addition a movement from Oz to PO7. We calculated the averaged and normalized topographical latency difference between Oz/O2 and O2/PO8 for all of the three components (this measure was termed ERP-TC) and correlated the obtained measures with the categorization-speed. We found a significant negative relationship (r = − 0.549) showing that short latency differences between Oz and PO8 were associated with slow picture-categorization

(cf. the scatter plot in Fig. 5A). In other words, a high travel speed was associated with a slow visual-semantic categorization process and a low speed with a fast categorization process. This finding suggests that a slow spreading activation process in the cortex reflects an intensive search for semantic contents which enhances semantic categorization.

Previous research particularly highlighted the role of upper alpha oscillations for semantic processing whereas lower alpha was associated with visual awareness and expectancy (e.g. Klimesch, 1999). It must be stressed that these results were mainly based on band-pass filtered data associated with ongoing mechanisms. When looking at event-related components and its relation to a certain evoked oscillatory activity (like the P1 in relation to alpha) it must be considered that other frequencies contribute to the generation of the P1 too. As an example Gruber et al. (2005) were able to show that the P1 is primarily related to phase-alignment in the alpha range but that there are other frequencies too, like theta and beta, which contribute to the generation and therefore influence the frequency-characteristic of the component. As a consequence the P1 must be seen as a superposition of different frequencies and it is unlikely that it consistently shows the dominance of a particular, narrow frequency. Nonetheless it is possible to demonstrate that the P1 and alpha-oscillations share the same functional role.

Mean topographical latency differences lay in the range of about 9 ms. The respective scalp distance between Oz, O2 and PO8 is about 60 mm. Thus, in terms of traveling speed in meter per second (TS = distance in mm/latency difference in ms) we obtain a value of about 6 m/s. This is twice as fast as observed in an earlier study from our lab (Klimesch et al., 2007a). According to Nunez et al. (2001) alpha phase velocities vary between about 6 and 14 m/s when considering a cortical folding factor of 2. Similar values were reported by Burkitt et al. (2000) who analyzed steady-state visual-evoked potentials and observed evoked traveling waves with a velocity ranging from 7 to 11. When considering this correction factor for our data we obtain a speed value of 12 m/s which marks the upper speed range for alpha.

Phase velocity depends on a variety of 'unspecific' (non-physiological) factors, such as recording methods (e.g. bipolar vs. referential recordings), measurement methods (e.g., MEG vs EEG) and frequency (cf. Nunez, 1995). Bipolar recordings give lower estimates than reference methods (as used in our study). Furthermore, measurements using MEG technology give even lower estimates. The disparity between these estimates may also be due in part to reference electrode and volume conduction effects. Frequency is also an important factor. For lower alpha (with a frequency of about 8 Hz) phase velocity is about 6 m/s, but for upper alpha (with a frequency of about 12 Hz) phase velocity is around 8 m/s (cf. Nunez, 1995, p. 568).

It is important to note that phase velocity also depends on the type of cognitive demands. As an example, in a study investigating alpha phase synchronization during the encoding of 'to-be-remembered' spoken words, Schack et al. (2003) found an average travel speed around 10 m/s. Most interestingly, travel speed was fastest for a neutral resting condition and faster for abstract than concrete words. Because abstract words are less numerous than concrete words, this may indicate that the search area can be narrowed down faster for abstract than for concrete words. It is worth mentioning that phase velocities as well as topographical patterns of phase synchronization showed differences between concrete and abstract words already in a very early time window of 100–200 ms. Only for concrete but not abstract words a distinct pattern of stable phase relations were obtained with a traveling direction from leading parieto-temporal to trailing anterior sites. One might speculate that the storage network for concrete words is larger and more intensely interconnected which causes a slowing down of the spreading activation process.

It should be emphasized that the relationship between traveling speed and classification speed (as measured by RTs) must be indirect.

If there would be a direct association, we would not only have to assume a positive correlation between travel speed and RT, but also that the RT-advantage for fast subjects is exactly of the same magnitude as that for travel speed. The speed differences of traveling waves lie in the range of about 2–10 ms, but those for RT's lie in the range of several 100 ms. Thus, the 'loss' in travel speed for subjects with short responses is negligible. Our interpretation is that it is the 'quality' of the more intense and complex spreading activation process that enhances the semantic classification process which in turn speeds up RT.

It should also be stressed that there may be an alternative (and not necessarily contradicting) interpretation of the behavioral data. This interpretation is suggested by the finding of the applied cluster analysis which led to the possible extraction of two subgroups of subjects (cf. Fig. 5C). Only those subjects with fast categorization-speed and a slow spreading activation process exhibited a travel speed that is consistent with the speed of alpha waves. Those subjects with slow picture-categorization had a travel speed that was much too fast for alpha. Thus, one might assume that only if traveling speed has been within the range that is characteristic for alpha oscillations, semantic categorization has operated under optimal conditions.

Our conclusion is that traveling evoked alpha waves reflect a spreading activation process that is functionally related to an access process to memory in a very similar way as the P1 may reflect early access to memory (see Klimesch, 2011 for a review). If these task demands are complex and difficult the spreading activation process is slowed down, if they are less complex and less difficult it is sped up. But what happens in a case when latency differences are not significant as was found for the presentation of the cue (cf. Fig. 3A)? To provide a possible answer to this question, we again refer to the hypothesis that the P1 is a manifestation of an inhibitory process that has two main purposes, to inhibit activation in task irrelevant networks and to control the SNR in task relevant networks. During the presentation of a cue the storage network is task irrelevant and the P1 reflects active inhibition to access the network. During the presentation of the picture the storage network is task relevant and the P1 reflects an inhibitory process that increases the SNR of the spreading activation process.

One of the most important general conclusions that can be drawn from the obtained findings is that alpha oscillations generate – or at least modulate – the early waveforms of the visual ERP. Single trial phase analysis has clearly shown that peaks and troughs in the alpha frequency range coincide with the N50, P1 and N1 (cf. Fig. 4). Even more important is the fact that topographical latency differences of the ERP components (i.e., the ERP-TC) can be explained by the respective topographical phase delays in the alpha – but not theta or beta – frequency range as suggested by the strong correlation between ERP-TC and alpha phase delay. The fact that the behavioral correlates with traveling speed and categorization-speed remained unchanged when phase delay instead of the ERP-TC was used emphasizes further that evoked alpha activity underlies the generation of the ERP waveform.

Appendix A. Supplementary data

Supplementary data to this article can be found online at doi:10.1016/j.neuroimage.2011.11.010.

References

Adrian, E.D., Matthews, B.H., 1934. The interpretation of potential waves in the cortex. J. Physiol. 81, 440–471.

Adrian, E.D., Yamagiwa, K., 1935. The origin of the Berger rhythm. Brain 58, 323–351.

Alexander, D.M., Trengove, C., Wright, J.J., Boord, P.R., Gordon, E., 2006. Measurement of phase gradients in the EEG. J. Neurosci. Methods 156, 111–128.

Allison, T., Puce, A., Spencer, D.D., McCarthy, G., 1999. Electrophysiological studies of human face perception. I: potentials generated in occipitotemporal cortex by face and non-face stimuli. Cereb. Cortex 9, 415–430.

Babiloni, C., Vecchio, F., Bultrini, A., Luca Romani, G., Rossini, P.M., 2006. Pre- and post-stimulus alpha rhythms are related to conscious visual perception: a high-resolution EEG study. Cereb. Cortex 16, 1690–1700.

Barry, R.J., 2009. Evoked activity and EEG phase resetting in the genesis of auditory Go/NoGo ERPs. Biol. Psychol. 80, 292–299.

Barry, R.J., de Pascalis, V., Hodder, D., Clarke, A.R., Johnstone, S.J., 2003. Preferred EEG brain states at stimulus onset in a fixed interstimulus interval auditory oddball task, and their effects on ERP components. Int. J. Psychophysiol. 47, 187–198.

Basar Eroglu, C., 1999. Brain function and oscillations. Vol. I: Principles and Approaches. Springer, Berlin.

Brandt, M.E., 1997. Visual and auditory evoked phase resetting of the alpha EEG. Int. J. Psychophysiol. 26, 285–298.

Brandt, M., Jansen, B., 1991. The relationship between prestimulus alpha-amplitude and visual evoked-potential amplitude. Int. J. Neurosci. 61, 261–268.

Burkitt, G.R., Silberstein, R.B., Cadusch, P.J., Wood, A.W., 2000. Steady-state visual evoked potentials and travelling waves. Clin. Neurophysiol. 111, 246–258.

Busch, N.A., Dubois, J., VanRullen, R., 2009. The phase of ongoing EEG oscillations predicts visual perception. J. Neurosci. 29, 7869–7876.

Di Russo, F., Martinez, A., Sereno, M.I., Pitzalis, S., Hillyard, S.A., 2002. Cortical sources of the early components of the visual evoked potential. Hum. Brain Mapp. 15, 95–111.

Ermentrout, G.B., Kleinfeld, D., 2001. Traveling electrical waves in cortex: insights from phase dynamics and speculation on a computational role. Neuron 29, 33–44.

Fell, J., Dietl, T., Grunwald, T., Kurthen, M., Klaver, P., Trautner, P., Schaller, C., Elger, C.E., Fernández, G., 2004. Neural bases of cognitive ERPs: more than phase reset. J. Cogn. Neurosci. 16, 1595–1604.

Fellinger, R., Klimesch, W., Gruber, W., Freunberger, R., Doppelmayr, M., 2011. Prestimulus alpha phase-alignment predicts P1-amplitude. Brain Res. Bull. 85, 417–423.

Freeman, W.J., 2004. Origin, structure, and role of background EEG activity. Part 1. Analytic amplitude. Clin. Neurophysiol. 115, 2077–2088.

Freunberger, R., Klimesch, W., 2008. EEG alpha oscillations and object recognition. Int. J. Psychol. 43, 451.

Freunberger, R., Holler, Y., Griesmayr, B., Gruber, W., Sauseng, P., Klimesch, W., 2008a. Functional similarities between the P1 component and alpha oscillations. Eur. J. Neurosci. 27, 2330–2340.

Freunberger, R., Klimesch, W., Griesmayr, B., Sauseng, P., Gruber, W., 2008b. Alpha phase coupling reflects object recognition. NeuroImage 42, 928–935.

Fuentemilla, L., Marco-Pallarés, J., Grau, C., 2006. Modulation of spectral power and of phase resetting of EEG contributes differentially to the generation of auditory event-related potentials. NeuroImage 30, 909–916.

Gruber, W.R., Klimesch, W., Sauseng, P., Doppelmayr, M., 2005. Alpha phase synchronization predicts P1 end N1 latency and amplitude size. Cereb. Cortex 15, 371–377.

Hanslmayr, S., Aslan, A., Staudigl, T., Klimesch, W., Herrmann, C.S., Bäuml, K.H., 2007. Prestimulus oscillations predict visual perception performance between and within subjects. NeuroImage 37, 1465–1473.

Hughes, J.R., 1995. The phenomenon of travelling waves: a review. Clin. Electroencephalogram 26, 1–6.

Itier, R.J., Taylor, M.J., 2004. N170 or N1? Spatiotemporal differences between object and face processing using ERPs. Cereb. Cortex 14, 132–142.

Klimesch, W., 1997. EEG-alpha rhythms and memory processes. Int. J. Psychophysiol. 26, 319–340.

Klimesch, W., 1999. EEG alpha and theta oscillations reflect cognitive and memory performance: a review and analysis. Brain Res. Rev. 29, 169–195.

Klimesch, W., 2011. Evoked alpha and early access to the knowledge system: the P1 inhibition timing hypothesis. Brain Res. 1408, 52–71.

Klimesch, W., Hanslmayr, S., Sauseng, P., Gruber, W.R., Doppelmayr, M., 2007a. P1 and traveling alpha waves: evidence for evoked oscillations. J. Neurophysiol. 97, 1311–1318.

Klimesch, W., Sauseng, P., Hanslmayr, S., 2007b. EEG alpha oscillations: the inhibition-timing hypothesis. Brain Res. Rev. 53, 63–88.

Klimesch, W., Sauseng, P., Hanslmayr, S., Gruber, W., Freunberger, R., 2007c. Event-related phase reorganization may explain evoked neural dynamics. Neurosci. Biobehav. Rev. 31, 1003–1016.

Klimesch, W., Fellinger, R., Freunberger, R., 2011. Alpha oscillations and early stages of visual encoding. Front. Psychol. 2.

Krieg, J., Trébuchon-Da Fonseca, A., Martínez-Montes, E., Marquis, P., Liégeois-Chauvel, C., Bénar, C.-G., 2011. A comparison of methods for assessing alpha phase resetting in electrophysiology, with application to intracerebral EEG in visual areas. NeuroImage 55, 67–86.

Kruglikov, S.Y., Schiff, S.J., 2003. Interplay of electroencephalogram phase and auditory-evoked neural activity. J. Neurosci. 23, 10122–10127.

Linkenkaer-Hansen, K., Palva, J.M., Sams, M., Hietanen, J.K., Aronen, H.J., Ilmoniemi, R.J., 1998. Face-selective processing in human extrastriate cortex around 120 ms after stimulus onset revealed by magneto- and electroencephalography. Neurosci. Lett. 253, 147–150.

Makeig, S., Westerfield, M., Jung, T.P., Enghoff, S., Townsend, J., Courchesne, E., Sejnowski, T.J., 2002. Dynamic brain sources of visual evoked responses. Science 295, 690–694.

Mäkinen, V., Tiitinen, H., May, P., 2005. Auditory event-related responses are generated independently of ongoing brain activity. NeuroImage 24, 961–968.

Mangun, G.R., Hinrichs, H., Scholz, M., Mueller-Gaertner, H.W., Herzog, H., Krause, B.J., Tellman, L., Kemna, L., Heinze, H.J., 2001. Integrating electrophysiology and neuro-imaging of spatial selective attention to simple isolated visual stimuli. Vis. Res. 41, 1423–1435.

Mathewson, K.E., Gratton, G., Fabiani, M., Beck, D.M., Ro, T., 2009. To see or not to see: prestimulus alpha phase predicts visual awareness. J. Neurosci. 29, 2725–2732.

Mazaheri, A., Jensen, O., 2006. Posterior alpha activity is not phase-reset by visual stimuli. Proc. Natl. Acad. Sci. U. S. A. 103, 2948–2952.

Mazaheri, A., Picton, T.W., 2005. EEG spectral dynamics during discrimination of auditory and visual targets. Cogn. Brain Res. 24, 81–96.

Mima, T., Oluwatimilehin, T., Hiraoka, T., Hallett, M., 2001. Transient interhemispheric neuronal synchrony correlates with object recognition. J. Neurosci. 21, 3942–3948.

Min, B.K., Busch, N.A., Debener, S., Kranczioch, C., Hanslmayr, S., Engel, A.K., Herrmann, C.S., 2007. The best of both worlds: phase-reset of human EEG alpha activity and additive power contribute to ERP generation. Int. J. Psychophysiol. 65, 58–68.

Nunez, P., 1995. Neocortical Dynamics and Human EEG Rhythms. Oxford University Press, New York.

Nunez, P.L., 2000. Toward a quantitative description of large-scale neocortical dynamic function and EEG. Behav. Brain Sci. 23, 371–398.

Nunez, P.L., Wingeier, B.M., Silberstein, R.B., 2001. Spatial-temporal structures of human alpha rhythms: theory, microcurrent sources, multiscale measurements, and global binding of local networks. Hum. Brain Mapp. 13, 125–164.

Oostenveld, R., Fries, P., Maris, E., Schoffelen, J.M., 2011. FieldTrip: open source software for advanced analysis of MEG, EEG, and invasive electrophysiological data. Comput. Intell. Neurosci. 156869 Article ID.

Ossandon, J.P., Helo, A.V., Montefusco-Siegmund, R., Maldonado, P.E., 2010. Superposition model predicts EEG occipital activity during free viewing of natural scenes. J. Neurosci. 30, 4787–4795.

Penny, W.D., Kiebel, S.J., Kilner, J.M., Rugg, M.D., 2002. Event-related brain dynamics. Trends Neurosci. 25, 387–389.

Petsche, H., Marko, A., 1955. Toposcopical studies on the extension of the alpha rhythm; preliminary report. Wien. Z. Nervenheilkd. Grenzgeb 12, 87–100.

Philiastides, M.G., Ratcliff, R., Sajda, P., 2006. Neural representation of task difficulty and decision making during perceptual categorization: a timing diagram. J. Neurosci. 26, 8965–8975.

Rajagovindan, R., Ding, M., 2010. From prestimulus alpha oscillation to visual-evoked response: an inverted-U function and its attentional modulation. J. Cogn. Neurosci. 23, 1379–1394.

Rihs, T.A., Michel, C.M., Thut, G., 2007. Mechanisms of selective inhibition in visual spatial attention are indexed by alpha-band EEG synchronization. Eur. J. Neurosci. 25, 603–610.

Risner, M.L., Aura, C.J., Black, J.E., Gawne, T.J., 2009. The Visual Evoked Potential is independent of surface alpha rhythm phase. NeuroImage 45, 463–469.

Ritter, P., Becker, R., 2009. Detecting alpha rhythm phase reset by phase sorting: caveats to consider. NeuroImage 47, 1–4.

Rizzuto, D.S., Madsen, J.R., Bromfield, E.B., Schulze-Bonhage, A., Seelig, D., Aschenbrenner-Scheibe, R., Kahana, M.J., 2003. Reset of human neocortical oscillations during a working memory task. Proc. Natl. Acad. Sci. U. S. A. (PNAS) 100, 7931–7936.

Romei, V., Gross, J., Thut, G., 2010. On the role of prestimulus alpha rhythms over occipito-parietal areas in visual input regulation: correlation or causation? J. Neurosci. 30, 8692–8697.

Sauseng, P., Klimesch, W., Gruber, W.R., Hanslmayr, S., Freunberger, R., Doppelmayr, M., 2007. Are event-related potential components generated by phase resetting of brain oscillations? A critical discussion. Neuroscience 146, 1435–1444.

Schack, B., Weiss, S., Rappelsberger, P., 2003. Cerebral information transfer during word processing: where and when goes it occur and how fast is it? Hum. Brain Mapp. 19, 18–36.

Shah, A.S., Bressler, S.L., Knuth, K.H., Ding, M., Mehta, A.D., Ulbert, I., Schroeder, C.E., 2004. Neural dynamics and the fundamental mechanisms of event-related brain potentials. Cereb. Cortex 14, 476–483.

Thut, G., Nietzel, A., Brandt, S.A., Pascual-Leone, A., 2006. Alpha-band electroencephalographic activity over occipital cortex indexes visuospatial attention bias and predicts visual target detection. J. Neurosci. 26, 9494–9502.

Vanni, S., Revonsuo, A., Hari, R., 1997. Modulation of the parieto-occipital alpha rhythm during object detection. J. Neurosci. 17, 7141–7147.

Wu, J.-Y., Huang, Xiaoying, Zhang, Chuan, 2008. Propagating waves of activity in the neocortex: what they are, what they do. Neuroscientist 14, 487–502.

Yamagishi, N., Callan, D.E., Goda, N., Anderson, S.J., Yoshida, Y., Kawato, M., 2003. Attentional modulation of oscillatory activity in human visual cortex. NeuroImage 20, 98–113.